HHS Public Access

Author manuscript

Phys Med Biol. Author manuscript; available in PMC 2015 April 17.

Published in final edited form as:

Phys Med Biol. 2008 May 21; 53(10): 2617–2631. doi:10.1088/0031-9155/53/10/012.

Incorporating a vascular term into a reference region model for the analysis of DCE-MRI data: a simulation study

A Z Faranesh[1] and **T E Yankeelov**[2,3]

[1] Department of Radiology, Stanford University, Stanford, CA 94305-5488, USA

[2] Institute of Imaging Science, Departments of Radiology and Radiological Sciences, Biomedical Engineering, Physics and Astronomy, Vanderbilt University, Nashville, TN, USA

Abstract

A vascular term was incorporated into a reference region (RR) model analysis of DCE-MRI data, and its effect on the accuracy of the model in estimating tissue kinetic parameters in a tissue of interest (TOI) was systematically investigated through computer simulations. Errors in the TOI volume transfer constant ($K^{trans,TOI}$) and TOI extravascular extracellular volume ($v_{e,TOI}$) that result when the fractional plasma volume (v_p) was included in (1) neither region, (2) TOI only (3) both regions were investigated. For nominal values of tumor kinetic parameters ($v_{e,TOI} = 0.40$ and $K^{trans,TOI} = 0.25\ min^{-1}$), if the vascular term was included in neither region or the TOI only, $K^{trans,TOI}$ error was within 20% for $0.03 < v_{p,TOI} < 0.10$, and $v_{e,TOI}$ error was within 20% for the range of $v_{p,TOI}$ studied (0.01–0.10). The effects of temporal resolution were shown to be complex, and in some cases errors increased with increasing temporal resolution.

Introduction

Dynamic contrast-enhanced MRI (DCE-MRI) can be used to characterize tumor physiology by tracking the movement of contrast media throughout the vasculature and tissue. It has been observed that tumor tissue displays different enhancement characteristics than normal tissue, and, in particular, it is believed that the rapid wash-in of contrast is due to the increased ‘leakiness’ of angiogenic tumor vasculature due to the larger gaps between endothelial cells (Fournier *et al* 2007, Kiessling *et al* 2007, Nakamura *et al* 2006, Provenzale *et al* 2006). Investigators have demonstrated that quantification of kinetic parameters in a DCE-MRI exam can be used to discriminate malignant and benign lesions (Chen *et al* 2006, Goto *et al* 2007, Kono *et al* 2007, Yankeelov and Gore 2007) and detect early treatment response in tumors (Lankester *et al* 2007, Wilmes *et al* 2007, Zahra *et al* 2007).

In a DCE-MRI exam, images are serially acquired during the intravenous administration of a bolus of a paramagnetic contrast agent. From the images the contrast agent concentration time course is calculated, and a pharmacokinetic model is used to extract parameters which

faranesh@nih.gov.

[3]Current address: National Heart, Lung, and Blood Institute, National Institutes of Health, 10 Center Drive, MSC 1538, Bldng 10, Rm 2C713, Bethesda, MD 20892-1538, USA.

characterize the concentration uptake curve. A commonly used model is the two-compartment pharmacokinetic model reviewed by Tofts *et al* (1999). The inputs to this model are the contrast agent concentrations in the vasculature (the so-called arterial or vascular input function) and tissue, and the fit parameters are the volume transfer constant (K^{trans}), the fractional extravascular extracellular (interstitial) volume (v_e), and the fractional plasma volume (v_p). The interstitial volume may increase in the case of either edema or cellular necrosis. The plasma volume is affected by changes in angiogenic activity and local hematocrit (Jain 1988). The physiological meaning of K^{trans} is complex, in that it relates to both the bulk flow and the permeability surface-area product of the tissue vasculature (Tofts *et al* 1999). It is generally believed that it correlates with the degree of tumor angiogenesis (Cha *et al* 2003, Montemurro *et al* 2007, Su *et al* 2003).

One of the primary challenges of DCE-MRI analysis is the accurate measurement of the plasma contrast agent concentration, often termed the arterial input function (AIF), which is used to drive the kinetic model. First, it is often difficult to achieve the temporal resolution (e.g. high sampling frequency) needed to accurately measure the AIF. For example, Henderson *et al* concluded that images must be acquired at least every second in order to accurately characterize plasma volume in the context of breast disease (Henderson *et al* 1998). Second, it is desirable to measure the AIF in close proximity to the tumor, and an appropriate vessel may not be in the field of view or it may be very small and difficult to image. Finally, vessel motion, flow and partial volume effects further confound accurate measurements of the AIF.

Models have recently been developed that enable the analysis of DCE-MRI data without having to characterize the time course of the contrast agent concentration in the plasma (Kovar *et al* 1998, Yang *et al* 2004, Yankeelov *et al* 2005). These ‘reference region’ methods do not yet account for the plasma volume contribution, though several investigators have pointed out its significance in tumor studies (Harrer *et al* 2004, Henderson *et al* 2000). The plasma volume in normal tissue is small and is therefore often ignored in DCE-MRI analysis. By comparison, the plasma volume in tumors and other pathological tissue may be quite large, possibly requiring explicit consideration. The primary goal of this work is to determine the effect of the vascular term on DCE-MRI analysis using the reference region model. In this work we explicitly incorporate a vascular term into the formalism and analyze, through simulations, its effect on the extracted pharmacokinetic parameters. By considering the inclusion of a vascular term in both the reference region (RR) and the tissue of interest (TOI) as the gold standard, we systematically investigated accuracy and precision in the extracted pharmacokinetic parameters that result when a vascular term was included in (1) neither region, (2) the TOI only and (3) in both regions in the presence of realistic experimental noise levels. The effect of temporal resolution was also investigated, by varying the sampling period from 1 to 30 s in the simulations. We conclude by making suggestions on when vascular terms should be incorporated if *a priori* knowledge concerning the range of tumor vascular volumes is known.

Theory

In the standard two-compartment model (Kety 1951, Larsson *et al* 1990, Tofts 1997, Tofts and Kermode 1991) the differential equation which describes the transport of contrast across the capillaries is given by

$$\frac{\mathrm{d}C_e(t)}{\mathrm{d}t} = \left(K^{trans}/v_e\right)\left(C_p(t) - C_e(t)\right), \quad (1)$$

where C_e and C_p are the contrast agent concentrations in the extravascular extracellular space and plasma space, respectively. The total tissue concentration, $C_t(t)$, is given by

$$C_t(t) = v_e C_e(t) + v_p C_p(t). \quad (2)$$

If the vascular contribution is neglected, then $C_p(t)$ may be calculated from $C_t(t)$ as

$$C_p(t) = \left(1/K^{trans}\right)\frac{\mathrm{d}}{\mathrm{d}t}C_t(t) + (1/v_e)\,C_t(t). \quad (3)$$

If the vascular term is included, then (see the appendix)

$$C_p(t) = (1/v_p)\,C_t(t) - \left(K^{trans}/(v_p)^2\right)\int_0^t C_t(u)\,\mathrm{e}^{-K^{trans}(1/v_p+1/v_e)(t-u)}\mathrm{d}u. \quad (4)$$

Using either equation (3) or equation (4), $C_p(t)$ may be calculated from a reference region of normal tissue (provided a reasonable estimate of K^{trans} and v_e of the reference tissue can be obtained) and used to drive the model in a tissue of interest to fit the kinetic parameters using equation (5):

$$C_t(t) = K^{trans}\int_0^t C_p(u)\,\mathrm{e}^{-\left(K^{trans}/v_e\right)(v_e)(t-u)}\mathrm{d}u + v_p C_p(t). \quad (5)$$

To improve computational efficiency, a linear form of equation (5) has been formulated by Murase (2004),

$$C_t(t) = \left(K^{trans} + \frac{K^{trams}}{v_e}v_p\right)\int_0^t C_p(u)\,\mathrm{d}u - \frac{K^{trans}}{v_e}\int_0^t C_t(u)\,\mathrm{d}u + v_p C_p(t). \quad (6)$$

In the tissue of interest, the vascular term may either be included or neglected by setting v_p to zero in equation (5) or equation (6). The plasma concentration is first calculated by either equations (3) or (4), and then substituted into equation (6) to calculate the concentration in the TOI.

Materials and methods

Simulations were run to determine the effects of including or excluding the vascular term on the accuracy and precision of the reference region model. The plasma concentration time course was defined by the functional form given by Parker *et al* (2006), which was derived from experimental data in patients acquired at a relatively high temporal resolution (4.97 s). In our work, we also assumed a nominal hematocrit of 0.42 (Kratz and Lewandrowski 1998). The initial time course value was subtracted off in order to set the initial point to zero, and a time step of 1 s was used.

Time courses for $C_{t,RR}(t)$ and $C_{t,TOI}(t)$ were synthesized using equation (5) with the following parameters: $K^{trans,RR} = 0.08\ min^{-1}$, $v_{e,RR} = 0.1$, $v_{p,RR} = 0.02$, $K^{trans,TOI} = 0.1–0.5\ min^{-1}$, $v_{e,TOI} = 0.1–0.5$ and $v_{p,TOI} = 0.01–0.10$. Varying amounts of noise were added to $C_{t,RR}(t)$ and $C_{t,TOI}(t)$, and $C_p(t)$ was calculated using either equation (3) (excluding $v_{p,RR}$) or equation (4) (including $v_{p,RR}$). The noise standard deviation was calculated as the maximum of $C_{t,RR}(t)$ divided by the desired signal-to-noise ratio (SNR). The kinetic parameters in the tissue of interest were calculated from the least-squares solution to equation (6), including and excluding the vascular term.

The tissue curves were analyzed in the following ways:

(1) $nv_{p,RR} - nv_{p,TOI}$: vascular term excluded from both regions (equations (3) and (6), with $v_p = 0$).

(2) $nv_{p,RR} - v_{p,TOI}$: vascular term excluded from reference region and included in tissue of interest (equations (3) and (6)).

(3) $v_{p,RR} - v_{p,TOI}$: vascular term included in both regions (equations (4) and (6)).

A series of 1000 Monte Carlo runs was performed and the per cent error was tabulated for each parameter.

In theory, the slower dynamics of the RR and TOI tissue time courses should allow a slower sampling rate to adequately characterize these curves, compared with the rate necessary to properly sample the plasma curve, thereby providing the opportunity to increase spatial resolution and/or signal-to-noise during data acquisition. To test this hypothesis, the tissue curves were sub-sampled at periods of 10, 20 and 30 s and the errors in all three parameters were calculated. For these simulations no noise was added to the curves, as we are interested in systematic errors.

Results

The simulated reference region tissue curve ($C_{t,RR}$) with the individual contributions of the plasma concentration (C_p) and extravascular extracellular concentration ($C_{e,RR}$) (see equation (2)) is shown in figure 1(a). Both C_p and $C_{e,RR}$ are weighted by their respective fractional volumes ($v_{p,RR}$ and $v_{e,RR}$). The plasma concentration contributes the initial peak in the tissue curve, while the extravascular extracellular concentration contributes the more gradual wash-in, plateau and wash-out phases. The calculated C_p curves are shown in figure 1(b). The actual value of C_p (solid line), C_p excluding $v_{p,RR}$ (equation (3)) (dashed line) and

C_p including v_{pRR} (equation (4)) (crosses) are shown. When the vascular term was excluded, large over- and undershoots resulted. If the vascular term was included, then the fit matched well with the actual value. The effects of increasing values of $v_{p,TOI}$ on $C_{t,TOI}$ are shown in figure 1(c). As $v_{p,TOI}$ increased, the initial slope, peak and plateau all increased in $C_{t,TOI}$.

We first explore the noise sensitivity for particular $K^{trans,TOI}$ and $v_{e,TOI}$ values and a range of $v_{p,TOI}$. The SNR sensitivity of the parameters is shown in figure 2 ($K^{trans,TOI}$ = 0.25 min^{-1}, $v_{e,TOI}$ = 0.40). If the vascular term was excluded from either the RR or TOI, then the errors in $K^{trans,TOI}$ and $v_{e,TOI}$ were stable for SNR > 40. For SNR = 60 and a nominal value of $v_{p,TOI}$ = 0.06, the $K^{trans,TOI}$ errors were: $nv_{p,RR} - nv_{p,TOI}$ = –4% and $nv_{p,RR} - v_{p,TOI}$ = –5%. If the vascular term was included in both regions ($v_{p,RR} - v_{p,TOI}$), then the error in $K^{trans,TOI}$ decreased monotonically with increasing SNR, from 14% (SNR = 10) to < 1% for SNR > 40.

The $v_{e,TOI}$ error exhibited similar trends as the $K^{trans,TOI}$ error, in that the values were stable for SNR > 40 if the vascular term was excluded from either the RR or TOI. For SNR = 60 and $v_{p,TOI}$ = 0.06, the $v_{e,TOI}$ errors were: $nv_{p,RR} - nv_{p,TOI}$ = –4% and $nv_{p,RR} - v_{p,TOI}$ = –4%. With the vascular term included in both regions, the $v_{e,TOI}$ error decreased from 5% to < 1% for SNR > 40.

The $v_{p,TOI}$ error showed a modest dependence on SNR for the $nv_{p,RR} - v_{p,TOI}$ case for values of $v_{p,TOI}$ > 0.04 and was approximately –100% for values of $v_{p,TOI}$ < 0.04. In the $v_{p,RR} - v_{p,TOI}$ case, the error in $v_{p,TOI}$ decreased exponentially with SNR, from approximately 35% (SNR = 10) to < 3% for SNR > 40.

We next present data on the dependence of parameter errors on the parameter values. Because the errors were relatively flat for SNR > 40, the SNR was fixed to 60 for the results described below, which examine the interdependence between the three parameters. Figure 3 shows contour plots for the error in $K^{trans,TOI}$ as a function of each parameter, for SNR = 60. For each column, one parameter was fixed, while the other two were varied. The fixed parameter values were $K^{trans,TOI}$ = 0.25 min^{-1}, $v_{e,TOI}$ = 0.40 and $v_{p,TOI}$ = 0.06 (Eliat 2004). Each row shows a different combination of including or excluding the vascular terms from the reference region and tissue of interest.

When the vascular term was excluded from the reference region and included in the tissue of interest ($nv_{p,RR} - v_{p,TOI}$), the vascular term was set to approximately zero by the least-squares fit (the *maximum* confidence interval for $v_{p,TOI}$ was [0.003, 0.005] in this case), resulting in a fit similar to the case where the vascular term was excluded from both regions ($nv_{p,RR} - nv_{p,TOI}$). This is likely due to the large peaks in the calculated AIF, as shown in figure 1(b).

If the vascular term was excluded from the reference region, the error in $K^{trans,TOI}$ crossed zero for certain parameter values. The error decreased with $K^{trans,TOI}$ and grew linearly with $v_{p,TOI}$. The slope of the error versus $v_{p,TOI}$ decreased with $K^{trans,TOI}$. The error was less sensitive to $v_{e,TOI}$, except for low values of $K^{trans,TOI}$ (< 0.25 min^{-1}), where the error decreased with $v_{e,TOI}$. For the nominal values $K^{trans,TOI}$ = 0.25 min^{-1} and $v_{e,TOI}$ = 0.40,

when the vascular term was excluded from the reference region then the errors in $K^{trans,TOI}$ were within 10% for $0.05<v_{p,TOI}<0.09$ and within 20% for $0.03<v_{p,TOI}<0.10$.

Figure 4 shows contour plots for the error in $v_{e,TOI}$ as a function of each parameter for SNR = 60. The error in $v_{e,TOI}$ was insensitive to $K^{trans,TOI}$. It decreased nonlinearly with $v_{e,TOI}$ and increased linearly by approximately 4% per 0.02 increase with $v_{p,TOI}$. As with the $K^{trans,TOI}$ error, the $v_{e,TOI}$ error crossed zero for certain parameter values when the vascular term was excluded from the reference region. For the nominal values $K^{trans,TOI} = 0.25\ min^{-1}$ and $v_{e,TOI} = 0.40$, when the vascular term was excluded from the reference region, then the $v_{e,TOI}$ errors were within 10% for $0.03 < v_{p,TOI} < 0.10$ and were within 20% for $0.01 < v_{p,TOI} < 0.10$.

Contour plots of the errors in $v_{p,TOI}$ for when the vascular term was excluded from the reference region are shown in figure 5. The errors in $v_{p,TOI}$ were close to –100% for all parameter values, meaning that the model set it to close to zero. This implies that the tissue of interest vascular term cannot be accurately estimated from the reference region model if the reference region vascular term is not included.

To evaluate how well the tissue of interest curve fit equation (6), the correlation coefficient, r^2, was calculated and is plotted in figure 6. When the vascular term was excluded from the reference region, $r^2 \geq 0.95$ for most parameter values, indicating a good fit to the model. For the nominal values of $K^{trans,TOI} = 0.25\ min^{-1}$ and $v_{e,TOI} = 0.40$, $r^2 > 0.95$ for $v_{p,TOI} > 0.02$.

Effects of temporal resolution

The effects of temporal resolution on $K^{trans,TOI}$ error are shown in figure 7. The sampling interval, Δt, was set to 1, 10, 20 and 30 s. This rate was used to sample the (noiseless) tissue curves in the reference region and tissue of interest, and the parameters were calculated as before, excluding or including the vascular term in each region. In each graph, one parameter was varied, while the other two were fixed at the following values: $K^{trans,TOI} = 0.25\ min^{-1}$, $v_{e,TOI} = 0.40$ and $v_{p,TOI} = 0.06$. The minimum and maximum parameter values are shown on each graph, with the curve corresponding to the minimum value shown as a dashed line.

When the vascular term was excluded from both regions ($nv_{p,RR} - nv_{p,TOI}$, first row), the $K^{trans,TOI}$ error was bounded by ±30% for the range of parameter values studied. The errors clustered at $\Delta t = 20$ s, where they exhibited little dependence on the parameter values. The $K^{trans,TOI}$ error became more negative with increasing Δt if the vascular term was included in only the tissue of interest ($nv_{p,RR} - v_{p,TOI}$). Compared with the $nv_{p,RR} - nv_{p,TOI}$ case, the errors varied over a wider range, and in several cases the error went from positive to negative as Δt increased, implying that the error was equal to zero for a particular sampling frequency. When the vascular term was included in both regions ($v_{pRR} - v_{p,TOI}$, third row), the errors began near zero and became more negative as Δt increased, as expected. The dependence on Δt was not linear and was different for each parameter. The dependence on $K^{trans,TOI}$ and $v_{e,TOI}$ was largest for $\Delta t = 20$ s. The sign of the dependence on $v_{p,TOI}$ reversed in going from $\Delta t = 10$ s to $\Delta t = 20$ s, seen as a ‘twist’ in the graph.

Figure 8 shows the error in $v_{e,TOI}$ as a function of the sampling period and each of the parameters. For the $nv_{pRR} - nv_{p,TOI}$ case, the $v_{e,TOI}$ error had little dependence Δt. If the vascular term was included in only the tissue of interest ($nv_{pRR} - v_{p,TOI}$), then the errors became more negative with Δt, but in some cases crossed zeros, as with the $K^{trans,TOI}$ error. When the vascular term was included in both regions the error began near zero then became more negative with Δt. Similar to the $K^{trans,TOI}$ error, the dependence on $v_{p,TOI}$ changes sign as Δt goes from 10 s to 20 s.

The influence of temporal resolution on $v_{p,TOI}$ error is shown in figure 9. For the $nv_{p,RR} - v_{p,TOI}$ case, the error became more positive with Δt, in some cases going from negative to positive. This dependence increased with $K^{trans,TOI}$, did not seem to depend on $v_{e,TOI}$ and decreased with $v_{p,TOI}$. For the $v_{p,RR} - v_{p,TOI}$ case, the $v_{p,TOI}$ error began near zero, increased for Δt = 10 s, then at Δt = 20 s increased for larger values of $K^{trans,TOI}$ and decreased for smaller values of $K^{trans,TOI}$. The $v_{p,TOI}$ error had less dependence on $v_{e,TOI}$, and peaked at Δt = 10 s, then decreased. For $v_{p,TOI} > 0.02$, the error had little dependence on Δt, but increased rapidly when Δt changes from 10 s to 20 s, for $v_{p,TOI} \leq 0.02$.

Discussion

In normal muscle tissue, the plasma contribution is approximately 1–2% (Faranesh *et al* 2006, Kuwatsuru *et al* 1993), and is often neglected in quantitative DCE-MRI. The fractional vascular volume may be significantly larger in tumors, and consequently may need to be considered in the kinetic model. For example, Harrer *et al* demonstrated in a study of patients with high grade gliomas (a highly vascularized tumor) that when the vascular term was not included in the kinetic model K^{trans} was overestimated by up to two orders of magnitude (Harrer *et al* 2004). In this work, the importance of the plasma term in calculating kinetic parameters from the reference region model was systematically analyzed.

If the vascular term was excluded from the reference region, then the errors in $K^{trans,TOI}$ crossed zero for particular combinations of the three parameters. In tumors or other environments that tend to be quite heterogeneous, this means that both the sign and magnitude of the error may be quite unpredictable; for example, for the values studied here, the error was in the range of [–42%, 71%].

Values for tumor $K^{trans,TOI}$, $v_{e,TOI}$ and $v_{p,TOI}$ vary widely in the literature (Henderson *et al* 2000), due to differences in tumor physiology, image acquisition protocols and analysis methods. It is still useful, however, to pick ‘typical’ values for these parameters to further examine the implications of the vascular term on DCE-MRI analysis. The fractional plasma volume ($v_{p,TOI}$) in tumors has been evaluated with macromolecular contrast agents such as albumin-GDTPA (Ogan *et al* 1987) or Gadomer-17 (Misselwitz *et al* 2001), which are currently only approved for use in pre-clinical studies. Using such agents, $v_{p,TOI}$ has been measured to be in the range of 0.045–0.0725 (Fournier *et al* 2007, Turetschek *et al* 2004) in human breast cancer xenograft studies. In a study of breast cancer in patients, Eliat *et al* measured $K^{trans,TOI} = 0.35 \pm 0.29$ min^{-1} and $v_{e,TOI}$ 0.43 ± 0.22 in malignant lesions, and $K^{trans,TOI}$ 0.14 ± 0.18 min^{-1} and $v_{e,TOI} = 0.49 \pm 0.29$ in benign lesions (Eliat 2004). Similar

values were also measured by Furman-Haran *et al* (Furman-Haran 2005). The choices of fixed TOI parameter values here are consistent with these studies.

The effects of temporal resolution on quantitative DCE-MRI have been investigated by several groups (Buckley 2002, Evelhoch 1999, Lopata 2007). With the two-compartment model, as the sampling period is increased, K^{trans} is underestimated and it becomes difficult to accurately measure v_p. In the reference region model, the effects of increasing the sampling period are more complx. Each of the terms in equation (6), $C_p(t)$ (calculated from the reference region), $\int_0^t C_p(\tau)\,d\tau$, and $\int_0^t C_{t,TOT}(\tau)\,d\tau$, is effected by the sampling period, which in turn effect the least-squares fit. When the sampling interval is made large enough to miss the initial peak in $C_{t,RR}$, the calculated C_p will not contain the large over- and undershoots seen in figure 1(a). This leads to unexpected results. For example, the absolute $K^{trans,TOI}$ error *decreased* when the sampling interval increased from 10 s to 20 s for the $nv_{p,RR} - nvp_{,TOI}$ case. In the $n\nu_{p,RR} - \nu_{p,TOI}$ case, the error decreased with increased sampling period, but in some cases it decreased from positive to negative, so that the absolute error was *reduced* for larger sampling intervals. In the $v_{p,RR} - v_{p,TOI}$ case, the errors in general decreased from zero in all cases as the sampling period increased, but the dependence was not straightforward, as with the sign reversal for $v_{p,TOI}$.

The physiology is best modeled if the vascular term is included in both regions, but this requires *a priori* knowledge of $v_{p,RR}$ and also introduces an additional degree of freedom in the fit, which will reduce the overall precision of the model. While the range of values of $v_{p,RR}$ in normal tissue is narrow, high temporal resolution (~ 1 s) is still needed since the *integrals* of C_p and C_t appear in the model solution (see equation (6)). With insufficient temporal resolution, these integral terms will be underestimated. In a model that includes the vascular term, the requirement for high temporal resolution for increased accuracy will impose greater limits on spatial resolution, slice coverage, and/or signal-to-noise, compared with a RR model that does not include the vascular term.

For the RR model without the vascular term, the errors may be acceptable at lower temporal resolutions, even for large ranges of $v_{p,TOI}$. For nominal values of $K^{trans,TOI} = 0.25\ min^{-1}$ and $v_{e,TOI} = 0.40$, the errors in $K^{trans,TOI}$ ranged from –27 to 17%, and the errors in $v_{e,TOI}$ ranged from –14 to –3% for the range of $v_{p,TOI}$ studied (0.01–0.10). If $v_{p,TOI} = 0.04$–0.08 (based on data in Fournier *et al* (2007) and Turetschek *et al* (2004)), the error ranges are small for $K^{trans,TOI}$ (–13 to 8%) and $v_{e,TOI}$ (–8 to –0%) for sampling periods up to 30 s.

In order for coarser sampling resolution to be sufficient, the magnitude of v_eC_e must be large compared with v_pC_p, especially during the first pass, so that the initial peak due to the vascular contribution does not contribute significantly to C_t. When the vascular term was excluded from the tissue of interest, the model increased $K^{trans,TOI}$ as $v_{p,TOI}$ increased in an attempt to fit $C_{t,TOI}$ (see figure 1(c)). In the $nv_{p,RR} - nv_{p,TOI}$ case, $K^{trans,TOI}$ is first underestimated to compensate for the large overshoots in the fitted C_p (see figure 1(b)), then overestimated to compensate for the contribution of $v_{p,TOI}$. The effect of $v_{e,TOI}$ is opposite that of $v_{p,TOI}$, in that the error in $K^{trans,TOI}$ *decreased* with increasing values of $v_{e,TOI}$. As $v_{e,TOI}$ increases, the relative contribution of $C_{e,RR}$ to $C_{t,RR}$ increases, decreasing the importance of the vascular contribution and the corresponding error in $K^{trans,TOI}$.

Errors in the kinetic parameter calculations will affect the diagnostic accuracy of tests designed to detect differences between malignant and benign lesions or response to treatment. For example, consider the data collected by Eliat *et al* (Eliat 2004). Assume that the true difference of means is 0.35–0.14 = 0.21, and n is equal to 50 in the malignant and benign groups, and $\alpha = 0.05$ for statistical significance. The power (1—probability of Type II error) of a two sample *t*-test test is quite high, 0.99 (Lenth 2006). If the $K^{trans,TOI}$ error is 30% (a conservative value for the $nv_{p,RR} - nv_{p,TOI}$ case), so that in the malignant lesions it is measured to be 0.25 (with the same SD), then the power is reduced to 0.61. Alternatively, to maintain the same power of 0.99, then the n for each group would have to be increased from 50 to 178.

In this work the effect of the vascular term and sampling period in the reference region model was investigated through computer simulations. The complex interdependence of $K^{trans,TOI}$, $v_{e,TOI}$ and $v_{p,TOI}$ was examined for different combinations of including the vascular term in the RR and TOI regions. If the vascular term was excluded from both regions, then the errors in $K^{trans,TOI}$ and $v_{e,TOI}$ were found to be within 30% for a large range of $K^{trans,TOI}$, $v_{e,TOI}$ and $v_{p,TOI}$. For nominal values of the kinetic parameters in the TOI ($K^{trans,TOI} = 0.25^{-1}$, $v_{e,TOI} = 0.40$), $K^{trans,TOI}$ errors are within 10% for $0.05 < v_{p,TOI} < 0.09$ and within 20% for $0.03 < v_{p,TOI} < 0.10$. For these nominal values $v_{e,TOI}$ errors are within 10% for $0.03 < v_{p,TOI} < 0.10$ and within 20% for $0.01 < v_{p,TOI} < 0.10$.

The effect of the sampling period was complex, and in some cases increasing the sampling period actually reduced the error in the parameter estimation. This investigation demonstrates that the vascular term may have significant effects which need to be considered in the reference region model analysis of DCE-MRI data.

Acknowledgments

We thank the Lucas Foundation and National Institutes of Health for financial support through T32 CA09695, U24 CA 126588 and 1K25 EB005936.

Appendix

Here we outline the calculation of the plasma concentration, C_p, from the tissue concentration with inclusion of the vascular term. For the Tofts two-compartment model, the differential equation which describes the change in contrast concentration in the extravascular, extracellular space is

$$\frac{dC_e}{dt} = \left(K^{trans}/v_e\right)(C_p - C_e). \quad \text{(A.1)}$$

The tissue concentration is a weighted sum of the concentrations in the two compartments:

$$C_t = v_e C_e + v_p C_p. \quad \text{(A.2)}$$

Solving for C_e gives

$$C_e = \frac{1}{v_e}\left(C_t - v_p C_p\right). \quad \text{(A.3)}$$

Substituting this expression into equation (A.1)

$$\frac{\mathrm{d}}{\mathrm{d}t}\left(C_t - v_p C_p\right) = K^{trans}\left[C_e - \frac{1}{v_e}\left(C_t - v_p C_p\right)\right] \quad \text{(A.4)}$$

equation (A.4) may be written as

$$\frac{\mathrm{d}y}{\mathrm{d}t} + ay = b\frac{\mathrm{d}f}{\mathrm{d}t} + cf, \quad \text{(A.5)}$$

with $y = C_p$, $f = C_t$, $a = K^{\text{trans}}(1/v_p + 1/v_e)$, $b = (1/v_p)$ and $c = (K^{\text{trans}}/v_p v_e)$.

Taking the Laplace transform of equation (A.5) and assuming $y(0) = 0$ and $f(0) = 0$,

$$Y(s) = bsF(s) \cdot \frac{1}{s+a} + cF(s) \cdot \frac{1}{s+a}, \quad \text{(A.6)}$$

where $Y(s)$ and $F(s)$ are the Laplace transforms of y and f, respectively.

Taking the inverse transform of equation (A.6), and denoting convolution by $\otimes$:

$$y = b\frac{\mathrm{d}f}{\mathrm{d}t} \otimes \mathrm{e}^{-at} + cf \otimes \mathrm{e}^{-at} \quad \text{(A.7)}$$

$$y = b\int_0^t \frac{\mathrm{d}f}{\mathrm{d}u}(u)\,\mathrm{e}^{-a(t-u)}\mathrm{d}u + c\int_0^t f(u)\,\mathrm{e}^{-a(t-u)}\mathrm{d}u. \quad \text{(A.8)}$$

After using integration by parts on the first term, we have

$$y = bf(t) + (c - ab)\int_0^t f(u)\,\mathrm{e}^{-a(t-u)}\mathrm{d}u. \quad \text{(A.9)}$$

Substituting our original terms back in and simplifying, we have

$$C_p = (1/v_p)\,C_t - \left(K^{trans}/(v_p)^2\right)\int_0^t C_t(u)\,\mathrm{e}^{-K^{trans}(1/v_p + 1/v_e)(t-u)}\mathrm{d}u \quad \text{(A.10)}$$

which is equation (4).

References

Buckley DL. Uncertainty in the analysis of tracer kinetics using dynamic contrast-enhanced T1-weighted MRI. Magn. Reson. Med. 2002; 47:601–6. [PubMed: 11870848]

Cha S, Johnson G, Wadghiri YZ, Jin O, Babb J, Zagzag D, Turnbull DH. Dynamic, contrast-enhanced perfusion MRI in mouse gliomas: correlation with histopathology. Magn. Reson. Med. 2003; 49:848–55. [PubMed: 12704767]

Chen W, Giger ML, Bick U, Newstead GM. Automatic identification and classification of characteristic kinetic curves of breast lesions on DCE-MRI. Med. Phys. 2006; 33:2878–87. [PubMed: 16964864]

Eliat PP-AD. Magnetic resonance imaging contrast-enhanced relaxometry of breast tumors: an MRI multicenter investigation concerning 100 patients. Magn. Reson. Imaging. 2004; 22:475–81. [PubMed: 15120166]

Evelhoch JL. Key factors in the acquisition of contrast kinetic data for oncology. J. Magn. Reson. Imaging. 1999; 10:254–9. [PubMed: 10508284]

Faranesh AZ, Kraitchman DL, McVeigh ER. Measurement of kinetic parameters in skeletal muscle by magnetic resonance imaging with an intravascular agent. Magn. Reson. Med. 2006; 55:1114–23. [PubMed: 16598733]

Fournier LS, Novikov V, Lucidi V, Fu Y, Miller T, Floyd E, Shames DM, Brasch RC. MR monitoring of cyclooxygenase-2 inhibition of angiogenesis in a human breast cancer model in rats. Radiology. 2007; 243:105–11. [PubMed: 17329684]

Furman-Haran EES. Magnetic resonance imaging reveals functional diversity of the vasculature in benign and malignant breast lesions. Cancer. 2005; 104:708–18. [PubMed: 15971199]

Goto M, Ito H, Akazawa K, Kubota T, Kizu O, Yamada K, Nishimura T. Diagnosis of breast tumors by contrast-enhanced MR imaging: comparison between the diagnostic performance of dynamic enhancement patterns and morphologic features. J. Magn. Reson. Imaging. 2007; 25:104–12. [PubMed: 17152054]

Harrer JU, Parker GJ, Haroon HA, Buckley DL, Embelton K, Roberts C, Baleriaux D, Jackson A. Comparative study of methods for determining vascular permeability and blood volume in human gliomas. J. Magn. Reson. Imaging. 2004; 20:748–57. [PubMed: 15503330]

Henderson E, Rutt BK, Lee TY. Temporal sampling requirements for the tracer kinetics modeling of breast disease. Magn. Reson. Imaging. 1998; 16:1057–73. [PubMed: 9839990]

Henderson E, Sykes J, Drost D, Weinmann HJ, Rutt BK, Lee TY. Simultaneous MRI measurement of blood, flow blood volume, and capillary permeability in mammary tumors using two different contrast agents. J. Magn. Reson. Imaging. 2000; 12:991–1003. [PubMed: 11105041]

Jain RK. Determinants of tumor blood flow: a review. Cancer research. 1988; 48:2641–58. [PubMed: 3282647]

Kety SS. The theory and applications of the exchange of inert gas at the lungs and tissues. Pharmacol. Rev. 1951; 3:1–41. [PubMed: 14833874]

Kiessling F, Morgenstern B, Zhang C. Contrast agents and applications to assess tumor angiogenesis in vivo by magnetic resonance imaging. Curr. Med. Chem. 2007; 14:77–91. [PubMed: 17266569]

Kono R, Fujimoto K, Terasaki H, Muller NL, Kato S, Sadohara J, Hayabuchi N, Takamori S. Dynamic MRI of solitary pulmonary nodules: comparison of enhancement patterns of malignant and benign small peripheral lung lesions. Am. J. Roentgenol. 2007; 188:26–36. [PubMed: 17179342]

Kovar DA, Lewis M, Karczmar GS. A new method for imaging perfusion and contrast extraction fraction: input functions derived from reference tissues. J. Magn. Reson. Imaging. 1998; 8:1126–34. [PubMed: 9786152]

Kratz A, Lewandrowski KB. Case records of the Massachusetts General Hospital. Weekly clinicopathological exercises. Normal reference laboratory values. N. Engl. J. Med. 1998; 339

Kuwatsuru R, Shames DM, Muhler A, Mintorovitch J, Vexler V, Mann JS, Cohn F, Price D, Huberty J, Brasch RC. Quantification of tissue plasma volume in the rat by contrast-enhanced magnetic resonance imaging. Magn. Reson. Med. 1993; 30:76–81. [PubMed: 8371678]

Lankester KJ, Maxwell RJ, Pedley RB, Dearling JL, Qureshi UA, El Emir E, Hill SA, Tozer GM. Combretastatin A-4-phosphate effectively increases tumor retention of the therapeutic antibody, 131I-A5B7, even at doses that are sub-optimal for vascular shut-down. Int. J. Oncol. 2007; 30:453–60. [PubMed: 17203228]

Larsson HB, Stubgaard M, Frederiksen JL, Jensen M, Henriksen O, Paulson OB. Quantitation of blood– brain barrier defect by magnetic resonance imaging and gadolinium-DTPA in patients with multiple sclerosis and brain tumors. Magn. Reson. Med. 1990; 16:117–31. [PubMed: 2255233]

Lenth, RV. [14 September 2007] Java Applets for Power and Sample Size [Computer software]. 2006. from http://www.stat.uiowa.edu/~rlenth/Power

Lopata RG. On the identifiability of pharmacokinetic parameters in dynamic contrast-enhanced imaging. Magn. Reson. Med. 2007; 58:425–9. [PubMed: 17654583]

Misselwitz B, Schmitt-Willich H, Ebert W, Frenzel T, Weinmann HJ. Pharmacokinetics of Gadomer-17, a new dendritic magnetic resonance contrast agent. MAGMA. 2001; 12:128–34. [PubMed: 11390268]

Montemurro F, Martincich L, Sarotto I, Bertotto I, Ponzone R, Cellini L, Redana S, Sismondi P, Aglietta M, Regge D. Relationship between DCE-MRI morphological and functional features and histopathological characteristics of breast cancer. Eur. Radiol. 2007; 17:1490–7. [PubMed: 17149623]

Murase K. Efficient method for calculating kinetic parameters using T1-weighted dynamic contrast-enhanced magnetic resonance imaging. Magn. Reson. Med. 2004; 51:858–62. [PubMed: 15065262]

Nakamura K, et al. KRN951, a highly potent inhibitor of vascular endothelial growth factor receptor tyrosine kinases, has antitumor activities and affects functional vascular properties. Cancer Res. 2006; 66:9134–42. [PubMed: 16982756]

Ogan MD, Schmiedl U, Moseley ME, Grodd W, Paajanen H, Brasch RC. Albumin labeled with Gd-DTPA. An intravascular contrast-enhancing agent for magnetic resonance blood pool imaging: preparation and characterization. Invest. Radiol. 1987; 22:665–71. [PubMed: 3667174]

Parker GJ, Roberts C, Macdonald A, Buonaccorsi GA, Cheung S, Buckley DL, Jackson A, Watson Y, Davies K, Jayson GC. Experimentally-derived functional form for a population-averaged high-temporal-resolution arterial input function for dynamic contrast-enhanced. MRI Magn. Reson. Med. 2006; 56:993–1000.

Provenzale JM, York G, Moya MG, Parks L, Choma M, Kealey S, Cole P, Serajuddin H. Correlation of relative permeability and relative cerebral blood volume in high-grade cerebral neoplasms. Am. J. Roentgenol. 2006; 187:1036–42. [PubMed: 16985154]

Su MY, et al. Correlation of dynamic contrast enhancement MRI parameters with microvessel density and VEGF for assessment of angiogenesis in breast cancer. J. Magn. Reson. Imaging. 2003; 18:467–77. [PubMed: 14508784]

Tofts PS. Modeling tracer kinetics in dynamic Gd-DTPA MR imaging. J. Magn. Reson. Imaging. 1997; 7:91–101. [PubMed: 9039598]

Tofts PS, Kermode AG. Measurement of the blood–brain barrier permeability and leakage space using dynamic MR imaging: 1. fundamental concepts. Magn. Reson. Med. 1991; 17:357–67. [PubMed: 2062210]

Tofts PS, et al. Estimating kinetic parameters from dynamic contrast-enhanced T(1)-weighted MRI of a diffusable tracer: standardized quantities and symbols. J. Magn. Reson. Imaging. 1999; 10:223–32. [PubMed: 10508281]

Turetschek K, Preda A, Novikov V, Brasch RC, Weinmann HJ, Wunderbaldinger P, Roberts TP. Tumor microvascular changes in antiangiogenic treatment: assessment by magnetic resonance contrast media of different molecular weights. J. Magn. Reson. Imaging. 2004; 20:138–44. [PubMed: 15221819]

Wilmes LJ, et al. AG-013736, a novel inhibitor of VEGF receptor tyrosine kinases, inhibits breast cancer growth and decreases vascular permeability as detected by dynamic contrast-enhanced magnetic resonance imaging. Magn. Reson. Imaging. 2007; 25:319–27. [PubMed: 17371720]

Yang C, Karczmar GS, Medved M, Stadler WM. Estimating the arterial input function using two reference tissues in dynamic contrast-enhanced MRI studies: fundamental concepts and simulations. Magn. Reson. Med. 2004; 52:1110–7. [PubMed: 15508148]

Yankeelov TE, Gore JC. Dynamic contrast enhanced magnetic resonance imaging in oncology: theory, data acquisition, analysis, and examples. Curr. Med. Imaging Rev. 2007; 3:91–107. [PubMed: 19829742]

Yankeelov TE, Luci JJ, Lepage M, Li R, Debusk L, Lin PC, Price RR, Gore JC. Quantitative pharmacokinetic analysis of DCE-MRI data without an arterial input function: a reference region model. Magn. Reson. Imaging. 2005; 23:519–29. [PubMed: 15919597]

Zahra MA, Hollingsworth KG, Sala E, Lomas DJ, Tan LT. Dynamic contrast-enhanced MRI as a predictor of tumour response to radiotherapy. Lancet Oncol. 2007; 8:63–74. [PubMed: 17196512]

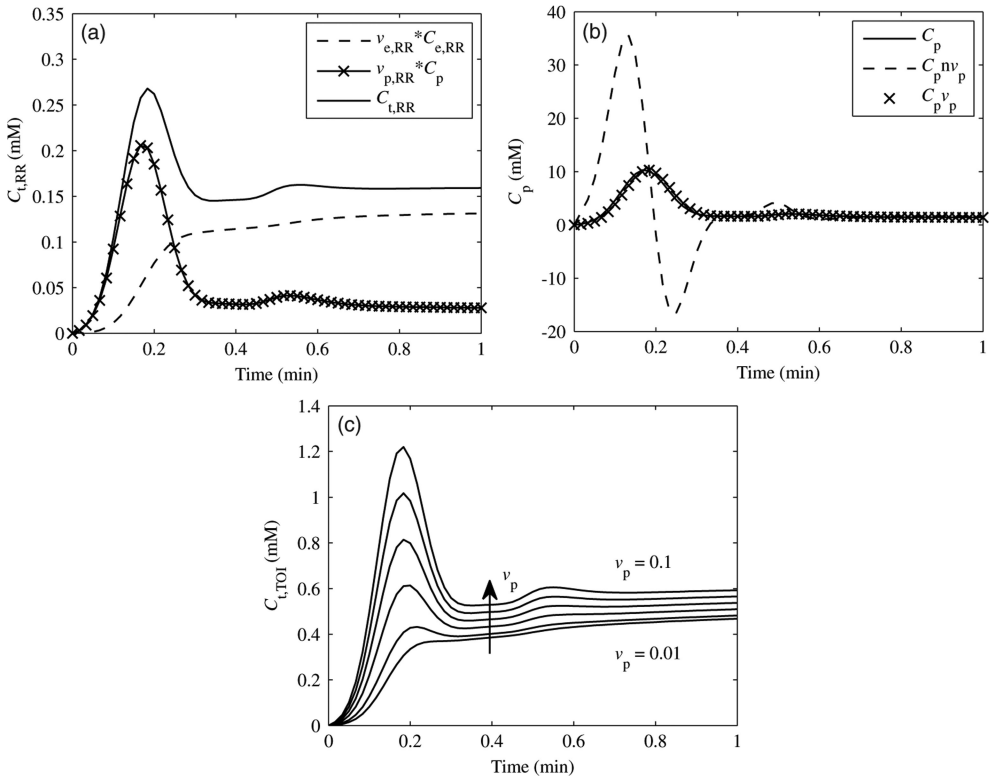

Figure 1.

(a) Contributions of C_p and $C_{e,RR}$ (each weighted by their respective fractional volumes) to $C_{t,RR}$, the reference region tissue concentration. (b) Resulting C_p curves from $C_{t,RR}$, excluding ($C_p n v_p$) or including ($C_p v_p$) the vascular term (see equations (3) and (4)). Note the large over- and undershoots when the vascular term was excluded. (c) Effect of $v_{p,TOI}$ on $C_{t,TOI}$. Curves are shown for values of $v_{p,TOI}$ increasing from 0.01 to 0.10.

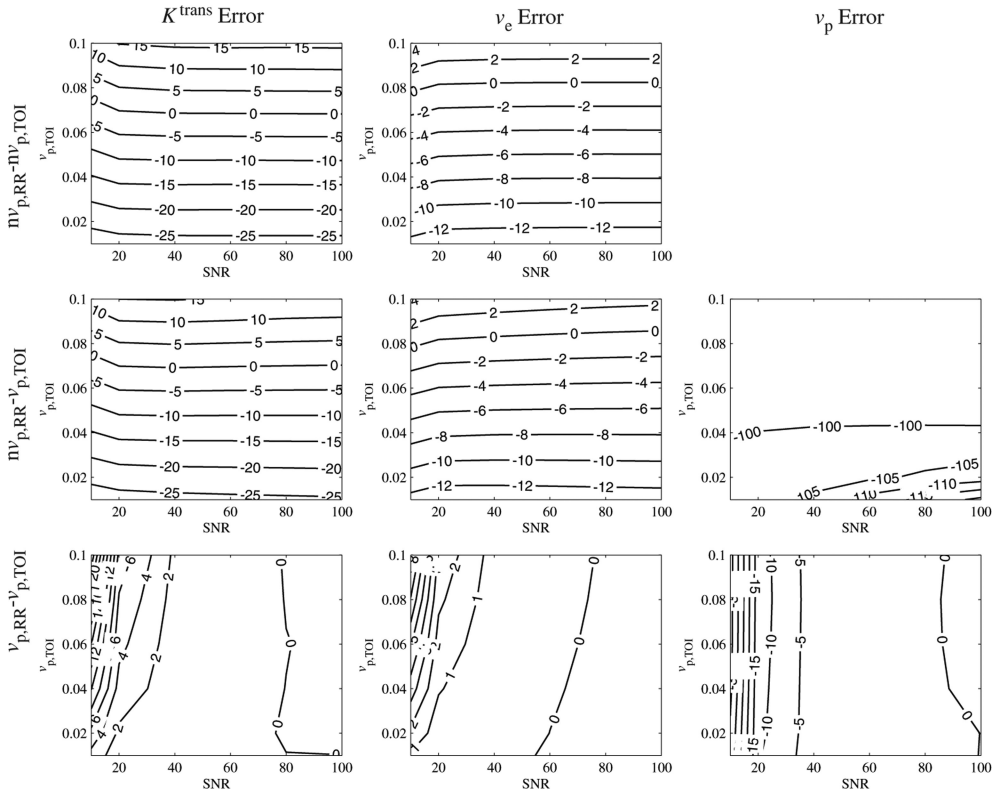

Figure 2.

Effect of SNR and $v_{p,TOI}$ on kinetic parameter errors, shown in per cent error. Errors were stable for SNR > 40, except for $v_{p,TOI} < 0.04$ in the $nv_{p,RR} - v_{p,TOI}$ case.

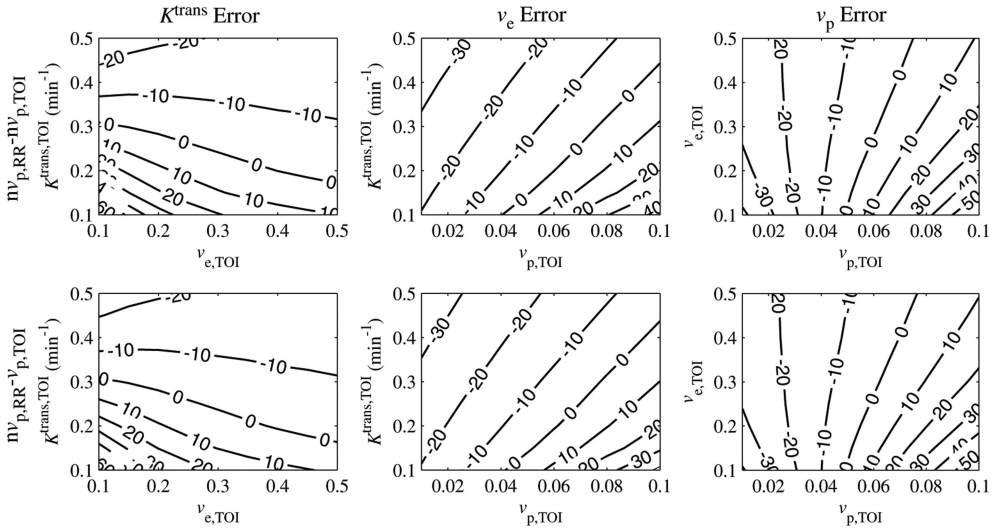

Figure 3.

$K^{trans,TOI}$ per cent error as a function of $K^{trans,TOI}$, $v_{e,TOI}$ and $v_{p,TOI}$. The errors intersected zero, indicating that the correct values awere estimated under certain conditions. The $K^{trans,TOI}$ error decreased with $K^{trans,TOI}$ and was relatively insensitive to $v_{e,TOI}$, although for low values of $K^{trans,TOI}$ it decreased with $v_{e,TOI}$. The error was linearly proportional to $v_{p,TOI}$.

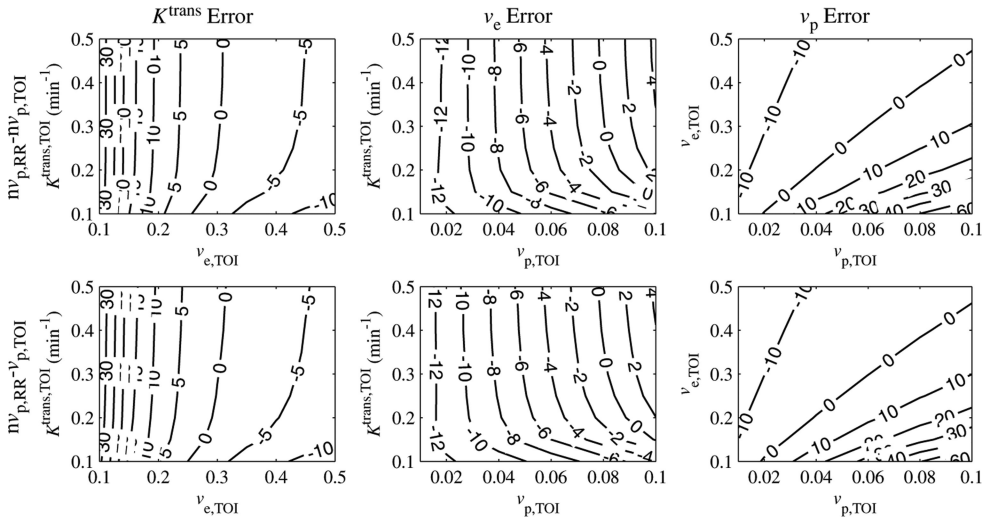

Figure 4.

$v_{e,TOI}$ per cent error as a function of $K^{trans,TOI}$, $v_{e,TOI}$ and $v_{p,TOI}$. The error intersected zero, indicating that the correct values were estimated under certain conditions. The $v_{e,TOI}$ error was relatively insensitive to $K^{trans,TOI}$ decreased nonlinearly with $v_{e,TOI}$ and increased linearly with $v_{p,TOI}$.

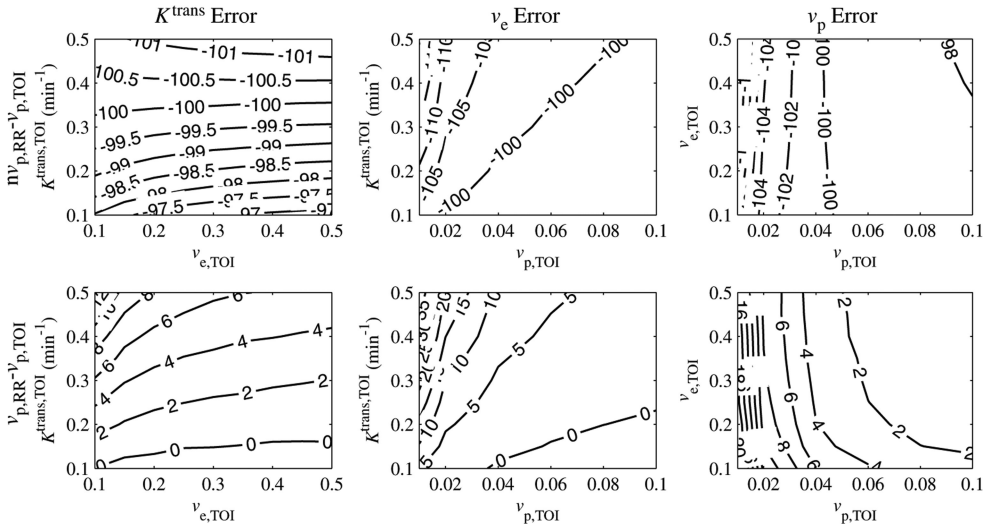

Figure 5.

$v_{p,TOI}$ error as a function of $K^{trans,TOI}$, $v_{e,TOI}$ and $v_{p,TOI}$. For the $nv_{p,RR} - v_{p,TOI}$ case, the error was close to –100%, reflecting the fact that the model set $v_{p,TOI}$ to close to zero even if it was included in the model. In the $v_{p,RR} - v_{p,TOI}$ case, the error increased linearly with $K^{trans,TOI}$, was insensitive to $v_{e,TOI}$ and decreased nonlinearly with $v_{p,TOI}$.

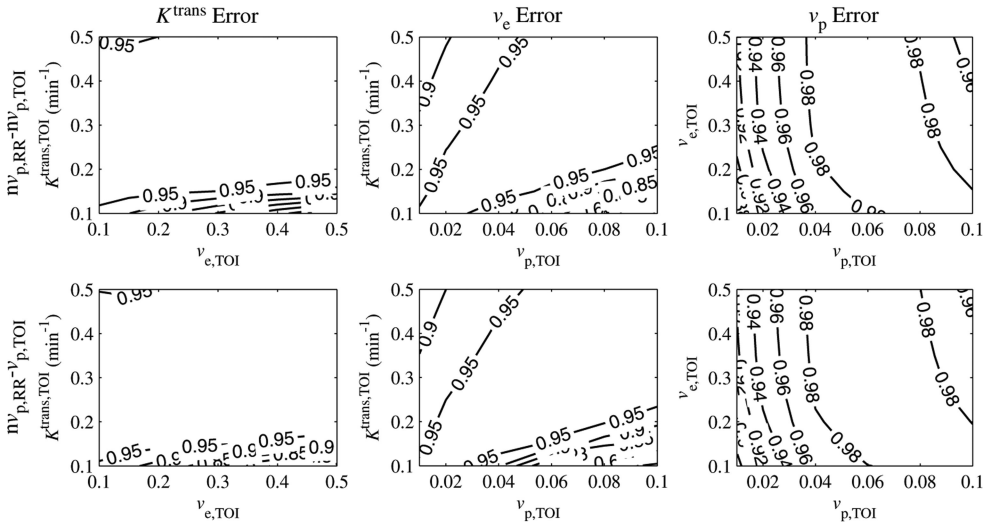

Figure 6.

r^2 goodness-of-fit statistic as a function of $K^{trans,TOI}$, $v_{e,TOI}$ and $v_{p,TOI}$. For most values, $r^2 >$ 0.9, except for regions of high $K^{trans,TOI}$, low $v_{p,TOI}$ and low $K^{trans,TOI}$, high $v_{p,TOI}$.

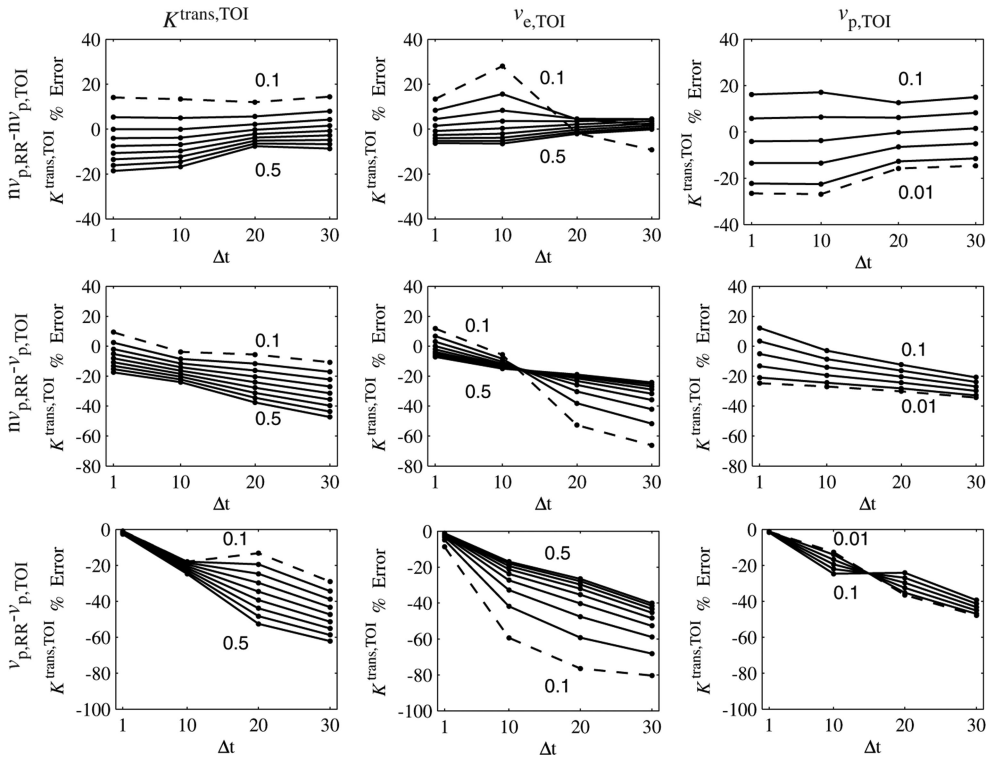

Figure 7.

$K^{trans,TOI}$ error as a function of sampling interval (Δt) and $K^{trans,TOI}$, $v_{e,TOI}$ and $v_{p,TOI}$. For each column, one parameter was varied, with the minimum and maximum parameter values shown in the graph (minimum shown as a dashed line). For the $nv_{p,RR} - nv_{p,TOI}$ case, the dependence on the parameter values reached a minimum at Δt = 20 s. For the $nv_{p,RR} - v_{p,TOI}$ case, the errors became more negative (sometimes crossing zero) as Δt increased. For the $v_{p,RR} - v_{p,TOI}$ case, the errors decreased from zero as Δt increased. The sign of the dependence on $v_{p,TOI}$ reversed when going from Δt = 10 s to Δt = 20 s.

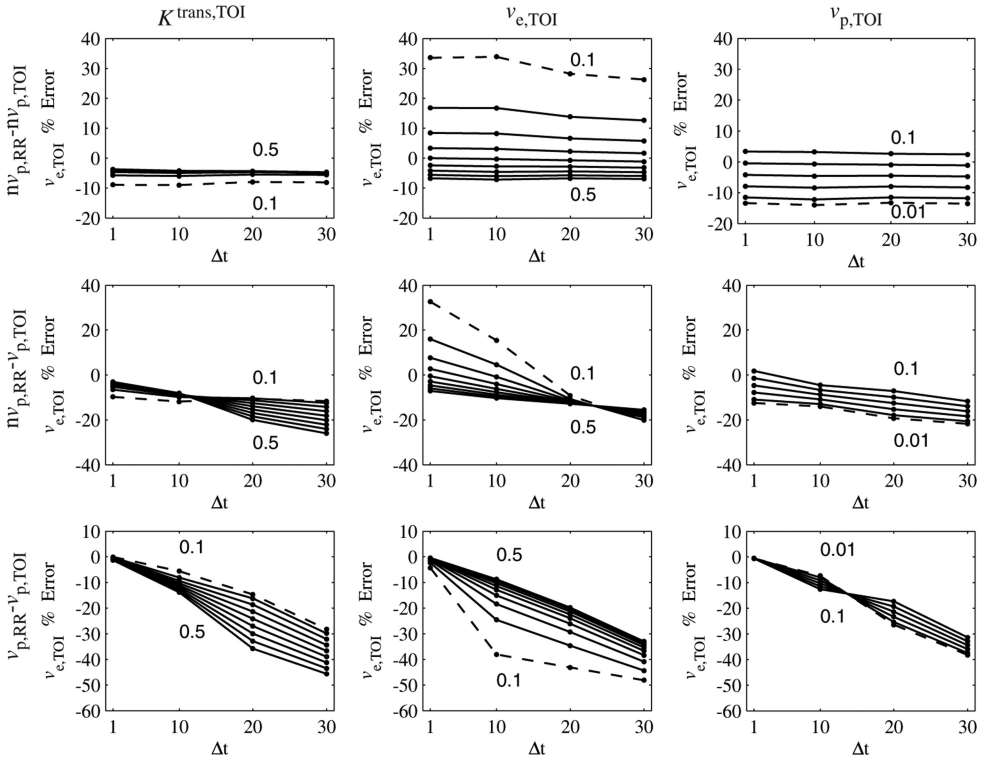

Figure 8.

Error in $v_{e,TOI}$ as a function of sampling rate (Δt) and $K^{trans,TOI}$, $v_{e,TOI}$ and $v_{p,TOI}$. For each column, one parameter was varied, with the minimum and maximum parameter values shown in the graph (minimum shown as a dashed line). For the $nv_{p,RR} - nv_{p,TOI}$ case, the errors were fairly insensitive to Δt. For the $nv_{p,RR} - v_{p,TOI}$ case, the errors became more negative (sometimes crossing zero) as Δt increased. For the $v_{p,RR} - v_{p,TOI}$ case, the errors decreased from zero as Δt increased. The sign of the dependence on $v_{p,TOI}$ reversed when going from Δt = 10 s to Δt = 20 s.

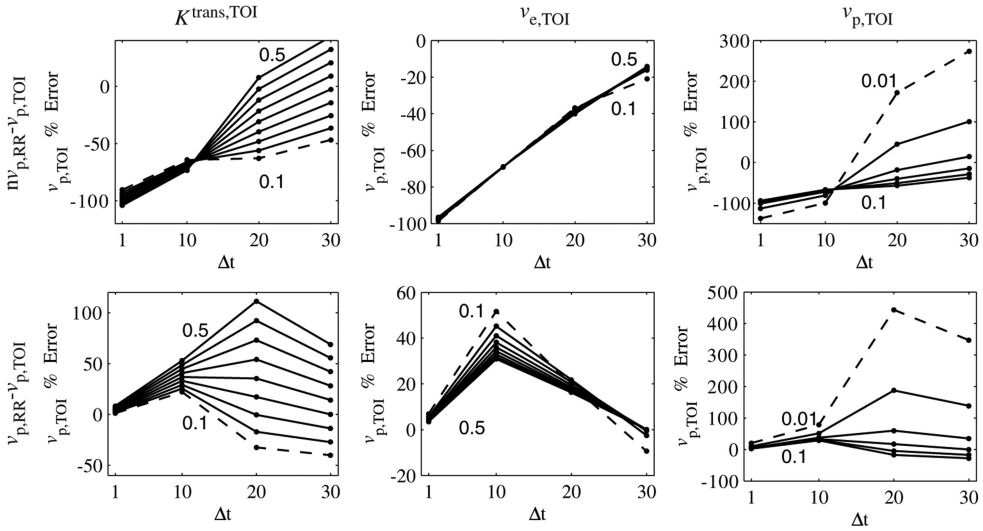

Figure 9.

Error in $v_{p,TOI}$ as a function of sampling rate (Δt) and $K^{trans,TOI}$, $v_{e,TOI}$ and $v_{p,TOI}$. For each column, one parameter was varied, with the minimum and maximum parameter values shown in the graph (minimum shown as a dashed line). For the $nv_{pRR} - v_{p,TOI}$ case the dependence on $K^{trans,TOI}$ increased with Δt, was insensitive to $v_{e,TOI}$ and decreased with $v_{p,TOI}$. For the $v_{pRR} - v_{p,TOI}$ case, the dependence on $K^{trans,TOI}$ and $v_{p,TOI}$ increased the most in going from Δt = 10 s to Δt = 20 s. The dependency on $v_{e,TOI}$ peaked at Δt = 10 s.